minerals

MDPI

Article

Simultaneous Biological and Chemical Removal of Sulfate and Fe(II)EDTA-NO in Anaerobic Conditions and Regulation of Sulfate Reduction Products

Yu Zhang *, Lijian Sun and Jiti Zhou

Key Laboratory of Industrial Ecology and Environmental Engineering (MOE), School of Environmental Science and Technology, Dalian University of Technology, Linggong Road 2, Dalian 116024, China; sunlijian_1993@163.com (L.S.); zjiti@dlut.edu.cn (J.Z.)

* Correspondence: zhangyu@dlut.edu.cn; Tel./Fax: +86-411-8470-6252

Received: 20 April 2019; Accepted: 24 May 2019; Published: 28 May 2019

Abstract: In the simultaneous flue gas desulfurization and denitrification by biological combined with chelating absorption technology, SO_2 and NO are converted into sulfate and Fe(II)EDTA-NO which need to be reduced in biological reactor. Increasing the removal loads of sulfate and Fe(II)EDTA-NO and converting sulfate to elemental sulfur will benefit the application of this process. A moving-bed biofilm reactor was adopted for sulfate and Fe(II)EDTA-NO biological reduction. The removal efficiencies of the sulfate and Fe(II)EDTA-NO were 96% and 92% with the influent loads of 2.88 kg $SO_4^{2-}\cdot m^{-3}\cdot d^{-1}$ and 0.48 kg $NO\cdot m^{-3}\cdot d^{-1}$. The sulfide produced by sulfate reduction could be reduced by increasing the concentrations of Fe(II)EDTA-NO and Fe(III)EDTA. The main reduction products of sulfate and Fe(II)EDTA-NO were elemental sulfur and N_2. It was found that the dominant strain of sulfate reducing bacteria in the system was *Desulfomicrobium*. *Pseudomonas*, *Sulfurovum* and *Arcobacter* were involved in the reduction of Fe(II)EDTA-NO.

Keywords: sulfate reduction; Fe(II)EDTA-NO reduction; Fe(III)EDTA; elemental sulfur; microbial community

1. Introduction

As a result of combusting fossil fuels, many contaminants, such as SO_2 and NO_x, may cause a series of environmental pollution like acid rain, photochemical smog and even the ozone layer destruction [1]. In recent times, the wide use of desulfurization and denitrification in flue gas have controlled SO_2 and NO_x at a relatively low level. However, shadows come with lights and the limestone/gypsum wet flue gas desulfurization (FGD) technology still has some shortages to overcome, especially economically, like energy consumption, process complexity and high cost during the process. In all of the FGD technology, selective catalytic reduction (SCR) is widely recognized, which consumes urea and ammonia to reduce NO_x in flue gas. However, to meet the high removal efficiency of NO_x, reducing agents should be added excessively, which means the excessive amount of ammonia will release into the air and cause secondary pollution [2]. At the same time, the biological flue gas desulfurization and denitrification technology has been gradually developed. Compared with the traditional process, the biological removal of SO_2 and NO_x from flue gas has the advantages of low energy consumption and operation cost, convenient operation, less secondary pollution and higher removal efficiency [3,4]. It mainly includes biological flue gas desulfurization technology (Bio-FGD) and the integrated physicochemical and biological technique for NO_x removal from flue gas (BioDeNOx, or chemical absorption biological reduction (CABR)).

Bio-FGD is a process in which SO_2 in flue gas is absorbed by alkaline solution to form sulfite or sulfate, then sulfite/sulfate is reduced to sulfide by sulfate-reducing bacteria (SRB) and sulfide

is oxidized to elemental sulfur by sulfide-oxidizing bacteria (SOB) [5,6]. BioDeNOx is that NO is absorbed by organic complexing absorbent, such as Fe(II)EDTA, and is converted into a complex absorption product (Fe(II)EDTA-NO) to realize the transfer of NO from the gas phase to liquid phase. Fe(II)EDTA-NO is then reduced to N_2 by microorganisms which use organic substances such as glucose or Fe(II)EDTA itself as an electron donor. Further, Fe(III)EDTA, oxidized by oxygen during absorption, can also be reduced by iron-reducing bacteria [7,8] (Equations (1)–(4)).

$$Fe(II)EDTA^{2-} + NO \rightarrow Fe(II)EDTA\text{-}NO^{2-} \quad (1)$$

$$12Fe(II)EDTA\text{-}NO^{2-} + C_6H_{12}O_6 \rightarrow 12Fe(II)EDTA^{2-} + 6CO_2 + 6N_2 + 6H_2O \quad (2)$$

$$2Fe(II)EDTA\text{-}NO^{2-} + 2Fe(II)EDTA^{2-} + 4H^+ \rightarrow 4Fe(III)EDTA + N_2 + 6H_2O \quad (3)$$

$$24Fe(III)EDTA^{-} + C_6H_{12}O_6 + 24OH^- \rightarrow 24Fe(II)EDTA^{2-} + 6CO_2 + 18H_2O \quad (4)$$

The combination of Bio-FGD and BioDeNOx technology may be a promising simultaneous flue gas desulfurization and denitrification technology. Simultaneous removal of SO_2 and NO in a rotating drum biofilter coupled with complexing absorption by Fe(II)EDTA has been reported [9,10]. These experiments studied the absorption and biotransformation of sulfur dioxide and nitric oxide in biofilters. The oxygen in the flue gas may affect the bioconversion process and it is difficult to control the final conversion product of sulfur dioxide. An integrated chemical and biological process has been proposed for simultaneous flue gas desulfurization and denitrification by our group. The process employs an alkaline Fe(II)EDTA solution to absorb SO_2 and NO from flue gas in a scrubber combined with biological reduction of the absorbed SO_2 utilizing sulfate reducing bacteria (SRB) and regeneration of the alkaline Fe(II)EDTA solution in a single bioreactor [11,12]. In batch experiments, Fe(III)EDTA, Fe(II)EDTA-NO and sulfate were simultaneously reduced by *Desulfovibrio* sp. CMX, which confirmed the feasibility of simultaneous transformation of flue gas desulfurization and denitrification products in a bioreactor [11,12]. The simultaneous removal of Fe(II)EDTA-NO and sulfate in an activated sludge anaerobic reactor has been studied. A large number of sulfides produced by sulfate reduction exist in the effluent of the reactor and need to be further treated [13].

For the process of simultaneous flue gas desulfurization and denitrification by alkaline Fe(II)EDTA solution combined with biological reduction of SO_2 and NO products in bioreactor, both Fe(II)EDTA-NO and Fe(III)EDTA produced in the process of NO absorption in flue gas have effects on the sulfide transformation produced by sulfate reduction in the anaerobic reactor. The nitrate-reducing, sulfide-oxidizing bacteria (NR-SOB) can be used for Fe(II)EDTA-NO and sulfide conversion. The autotrophic denitrification of Fe(II)EDTA-NO by sulfide has been reported [14]. The chemical reaction of Fe(III)EDTA with sulfide has been fully studied in the treatment of hydrogen sulfide tail gas [15,16]. In the process of absorbing SO_2 and NO in flue gas with Fe(II)EDTA, the concentrations of Fe(II)EDTA-NO, Fe(III)EDTA and sulfate in the solution vary with SO_2 concentration, NO concentration, oxygen content and Fe(II)EDTA concentration. Therefore, it is significant to convert sulfide produced by sulfate reduction into elemental sulfur by controlling the concentrations of Fe(II)EDTA-NO, Fe(III)EDTA and sulfate in the influent of the bioreactor.

In recent years, moving-bed biofilm reactor (MBBR) has been widely used in the fields of sulfate reduction, sulfur autotrophic denitrification, nitrification and denitrification due to its comparatively low footprint and efficient treatment performance [17,18]. The MBBR process principle is based on the basic principle of the biofilm process, making full use of the advantages of the activated sludge process and overcoming the shortcomings of the traditional activated sludge process and the fixed biofilm process. Yuan et al. found that while the NO_3^--N was 12.6 mg·L^{-1}, the highest NO_3^--N removal rate of MBBR filled with polyethylene carriers was 96% [19]. The sulfur-oxidizing autotrophic denitrification in MBBR achieved the nitrogen removal efficiency of 94% at the volumetric loading rate of 0.18 kg N·m^{-3}·d^{-1} [17]. Nitrate and sulfate can be effectively reduced in MBBR, so it is suitable for simultaneous removal of sulfate and Fe(II)EDTA-NO.

In this study, MBBR was adopted in order to improve the reduction load of sulfate and Fe(II)EDTA-NO produced in the simultaneous flue gas desulfurization and denitrification process. Reactor operation was divided into seven stages. After the start-up period, the treatment load of the reactor was increased by increasing the influent concentration of sulfate and Fe(II)EDTA-NO and reducing HRT (hydraulic retention time). The transformation of sulfate and Fe(II)EDTA-NO was studied by analyzing the concentration of sulfate, thiosulfate, sulfide, Fe(II)EDTA-NO, total iron and ferrous iron in the reactor effluent. By increasing the concentration of Fe(II)EDTA-NO and Fe(III)EDTA and controlling the concentration of sulfate in the influent of the reactor, the transformation from sulfate to sulfide and finally to elemental sulfur was completed in a reactor. The characteristics of functional bacteria and the change of functional bacteria with reaction conditions were found by analyzing the microbial communities in different operation stages of the reactor.

2. Materials and Methods

2.1. Experimental Materials

2.1.1. Experimental Device

The reactor was an anaerobic moving-bed biofilm reactor (MBBR) with a diameter of 150 mm, a total height of 250 mm and an effective volume of 3.5 L. The reactor was equipped with an agitator, and the two groups of agitator blades were located, respectively, 70 mm and 140 mm away from the bottom. The outer ring of the reactor was equipped with a water bath interlayer. The interlayer used a water bath pot to control the temperature at 30 °C. The bottom of the reactor was equipped with a purge-head which could aerate nitrogen to the reactor, thus making the reactor anaerobic. Cylindrical polyethylene fillers with 10 mm in diameter and 10 mm in height were used in the reactor. The specific surface area of each of the fillers was 500 m^2/m^3 and the filling rate of the filler in the reactor was 30%. The inoculated sludge was the sludge from the secondary clarifier of Lingshui Sewage Treatment Plant in Dalian. After sieving, 2.5 L sludge was added into the reactor. The volatile suspended solids (VSS) of the sampled sludge was 14.5 $g{\cdot}L^{-1}$. The influent was fed into the bottom of the reactor by a peristaltic pump.

2.1.2. Influent Quality

The influent used in the experiment was manually prepared, and the water intake in the start-up stage was as follows: 10 mM Na_2SO_4; 2 mM $NaNO_3$; 1.13 mM Fe(II)EDTA. Mineral quality: yeast powder, 1 $g{\cdot}L^{-1}$; K_2HPO_4, 0.5 $g{\cdot}L^{-1}$; $MgCl_2$, 1.0 $g{\cdot}L^{-1}$; NH_4Cl, 1.0 $g{\cdot}L^{-1}$; $CaCl_2$, 0.1 $g{\cdot}L^{-1}$; $NaHCO_3$, 0.5 $g{\cdot}L^{-1}$. In other stages of the reaction, the concentrations of sulfate were 10–25 mM.

Then, 1 mL of trace element solution was added to each liter of influent water: $(NH_4)_6Mo_7O_{24}{\cdot}4H_2O$, 1.10 $g{\cdot}L^{-1}$; EDTA$\cdot 2H_2O$, 55.35 $g{\cdot}L^{-1}$; $ZnSO_4{\cdot}7H_2O$, 39.16 $g{\cdot}L^{-1}$, $CaCl_2$, 5.54 $g{\cdot}L^{-1}$; $MnSO_4{\cdot}H_2O$, 6.79 $g{\cdot}L^{-1}$; $FeSO_4{\cdot}7H_2O$, 9.13 $g{\cdot}L^{-1}$; $CuSO_4{\cdot}H_2O$, 2.45 $g{\cdot}L^{-1}$; $CoCl_2{\cdot}6H_2O$, 2.95 $g{\cdot}L^{-1}$ [13].

From the third stage, Fe(II)EDTA-NO solution was prepared with buffer solution of pH = 7 which had concentrations of 2–8 mM. The Fe(II)EDTA-NO solution was added into the reactor with the influent through a peristaltic pump. The preparation of Fe(III)EDTA solution referred to the original method where the concentrations were 4–6 mM [20].

2.2. Analysis Method

The pH value was measured with pH meter (Mettlertoledo, FE20). Fe(II) and total Fe were measured with the o-phenanthroline method. Sulfide was measured with Methylene Blue Spectrophotometry. NO_3^-, NO_2^-, $S_2O_3^{2-}$ and SO_4^{2-} were measured with ion chromatography (Dionex, ICS-1100). Fe(II)EDTA-NO was measured at 438 nm by Spectrophotometry (Mapada, UV-6100). N_2 and N_2O in gas phase were measured with gas chromatography (Techcomp, GC7900).

The content of hydrogen sulfide was measured with the zinc acetate absorption method. VSS was determined according to the standard methods [21].

2.3. High Throughput Sequencing

Firstly, the filler was put into the lysing agent to break the cell wall and release DNA. DNA extraction from sludge samples was performed using OMEGA DNA isolation kit (M5635-02, Sangon Biotech Co., Ltd. Shanghai, China). The integrity of DNA was detected by agarose gel and the extracted DNA was checked by electrophoresis on 1% agarosegel. Next, the extracted DNA was amplified by PCR. The following primer sets were used for PCR amplification: forward primer 341F and reverse primer 805R. The PCR amplification was performed in 0.1 mL reaction tubes using the following program: 3 min at 94 °C, five cycles (30 s at 94 °C, 20 s at 45 °C, 30 s at 65 °C), 20 cycles (20 s at 94 °C, 20 s at 55 °C, 30 s at 65 °C) and 5 min at 72 °C. Then, 3 min at 94 °C, five cycles (20 s at 94 °C, 20 s at 55 °C and 30 s at 72 °C). Purified PCR products was checked by electrophoresis on 2% agarosegel with UV emission. Then, DNA was purified and recovered. For bacterial amplified PCR products and normal amplified fragments over 400 BP of PCR products, 0.6 times of magnetic beads (Agencourt AMPure XP) were used to treat them. Qubit 3.0 DNA detection kit (Q10212, Life Technologies Corporation, Beijing, China) was used to quantify the recovered DNA accurately so as to facilitate mixing and sequencing according to 1:1 equivalence. When mixed equally, the DNA content of each sample was 10 ng and the final sequencing concentration was 20 pmol.

3. Results and Discussion

3.1. Simultaneous Biological and Chemical Removal of Sulfate and Fe(II)EDTA-NO in MBBR and Regulation of Sulfate Reduction Products

The reactor operation could be divided into seven stages according to the different reaction parameters. The operating parameters of each stage of the reactor are shown in Table 1.

Table 1. Reactor stage parameters.

Reaction Stage	Sulfate Concentration/mM	Fe(II)EDTA-NO Concentration/mM	HRT/h	Fe(III)EDTA Concentration/mM	Nitrate Concentration/mM	Run Time/d
Stage 1	10	0	48	0	2	32
Stage 2	10	0–2	24	0	2–0	24
Stage 3	15–25	2.5–3	24–20	0	0	61
Stage 4	25	3.5–8	20	0	0	70
Stage 5	25	8	20	4–6	0	27
Stage 6	20–15	8	16–12	6	0	54
Stage 7	15	8	12	6	0	12

The first stage was the start-up stage of biofilm formation. Many researchers have found that the process of biofilm formation on filler surface could be frequently affected by the environmental and operational conditions, such as carbon and nutrients availability, fluid velocity, MLSS, temperature, pH and surface roughness [22]. It has been proved that the formation of biofilms is very slow at the initial stage in the removal of pollutants in MBBR [23]. Their results showed that the planktonic cells first adhered to the filler loosely, then the cells gathered and grew on the surface of the filler to form a biofilm and the biofilm formation rate increased with the decrease of HRT. In the first stage, the HRT was 48 h. The concentration of sulfate in the influent was 10 mM and 2 mM nitrate was used instead of Fe(II)EDTA-NO. The agitator and aerator were closed to ensure the film-forming of sulfate reducing bacteria and denitrifying bacteria on the filler surface. After 20 days of reactor operation, the removal efficiency of sulfate could reach more than 95% (Figure 1) and the colonization of sulfate reducing bacteria was successful. The film-forming on the filler was unsatisfactory and a lot of activated sludge was suspended in the reactor. After 10 days of continuous culture, a layer of biofilm was observed on the inner surface of the filler which was black with a thickness of about 0.5 mm. The amount of suspended sludge was very small in the reactor. Combined with the reduction of suspended sludge in

the solution and the formation of biofilm on the filler surface, it was proved that biofilm formation was successful. At this time, the removal rates of sulphate and nitrate remained at the previous high levels. In the subsequent reactor operation, the reactor HRT was reduced and the influent load was increased to improve the reactor treatment load. No thiosulfate had been detected in the effluent from the reactor start-up. In this stage, the average sulfide concentration in effluent was 5.42 mM and 53.7% of the sulfate reduction products were sulfides. The sulfur autotrophic denitrification reaction with sulfide as the electron donor and nitrate as the electron acceptor is shown in Equation (5) [24]. More specifically, 2 mM nitrate can convert up to 5 mM sulfide into elemental sulfur. Therefore, sulfide existed in the effluent of the reactor when the sulfate was almost completely degraded.

$$S^{2-} + 0.4NO_3^- + 2.4H^+ = S_0 + 0.2N_2 + 1.2H_2O \quad (5)$$

In the second stage, HRT was reduced to 24 h. The sulfate removal efficiency was reduced to 70% at the initial adjustment stage and then was quickly recovered to more than 90% (Figure 1). From the 41st day, 2 mM Fe(II)EDTA-NO was added into the intake water. The removal efficiency of sulfate was greatly affected by the addition of Fe(II)EDTA-NO, which inhibited the activity of sulfate-reducing bacteria and led to the decrease of the removal efficiency. Chen et al. confirmed that adding 2.5 mM of Fe(II)EDTA-NO into sulfate reduction system could inhibit the sulfate reduction ability of sulfate reducing bacteria, and the inhibition effect was related to the Fe(II)EDTA-NO concentration [11]. After eight days of operation, sulfate removal efficiency increased and the average removal efficiency was 93.6%. When Fe(II)EDTA-NO was added to the reactor, it could quickly achieve better removal and the Fe(II)EDTA-NO removal efficiency reached 93.3% (Figure 2). In this stage, the sulfide concentration in the effluent was not affected by the decrease of HRT. However, the sulfide concentration tended to increase after the Fe(II)EDTA-NO replaced nitrate in the influent.

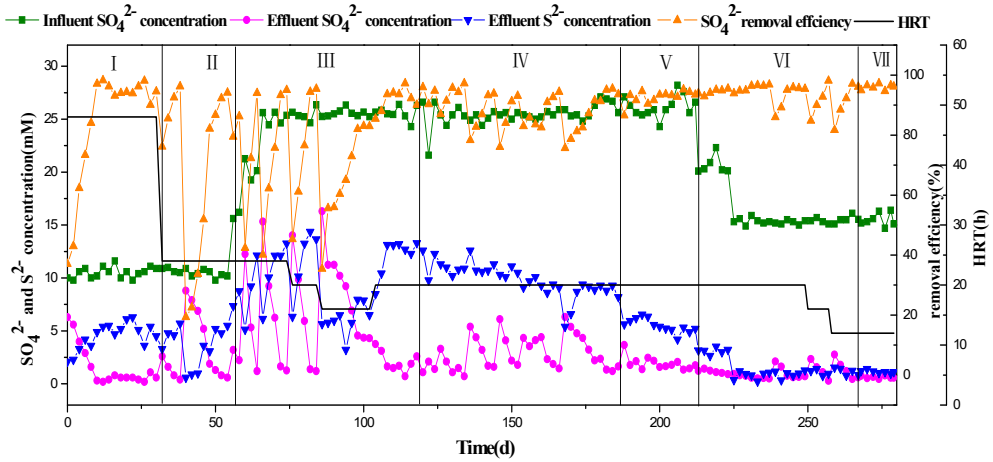

Figure 1. The concentrations of sulfate and sulfide in the influent and effluent and the sulfate removal efficiency.

In the third stage, the sulfate and Fe(II)EDTA-NO removal loads were increased by increasing the concentration of sulfate and Fe(II)EDTA-NO in the influent and reducing HRT. Firstly, the influent concentrations of sulfate and Fe(II)EDTA-NO were increased by 5 mM and 0.5 mM at a time. In this process, the removal efficiency of sulfate and Fe(II)EDTA-NO remained at about 95% and 92%, respectively (Figures 1 and 2). Manconi et al. found that the concentration of sulfate and sulfite did not affect the removal efficiency of Fe(II)EDTA-NO at higher sludge concentration [14]. The sulfide produced by sulfate reduction increased with the increase of sulfate concentration, accounting for 50–60% of total sulfate removal. Sulfide and Fe(II)EDTA-NO may undergo sulfur autotrophic denitrification and even direct chemical reaction to produce elemental sulfur [25]. Hydrogen sulfide and ferrous sulfide may be produced with the increase of sulfide concentration in the reactor. Chen et al.

found that many sulfides produced by sulfate reduction existed in the form of hydrogen sulfide in simultaneous removal of SO_2 and NO in a rotating drum biofilter [9,10]. Both Zhou et al. [26] and Xia et al. [27] observed the formation of FeS in the sulfate reduction system containing ferric iron. When the sulfate concentration was increased to 25 mM, the sulfate removal efficiency was more affected and would take a long time to recover to more than 90%. Therefore, the influent concentration of SO_4^{2-} was not increased and remained at 2.4 g/L. In the experiment of simultaneous removal of sulfate and Fe(II)EDTA-NO in anaerobic activated sludge reactor, the maximum influent concentration of sulfate was only 0.96 g/L [13]. Saritpongteeraka et al. used two anaerobic baffled reactors to treat high sulfate wastewater where the concentration of sulfate in the raw wastewater could reach 1819 ± 483 mg/L [28]. It can be seen that MBBR can adapt to higher influent sulfate concentration.

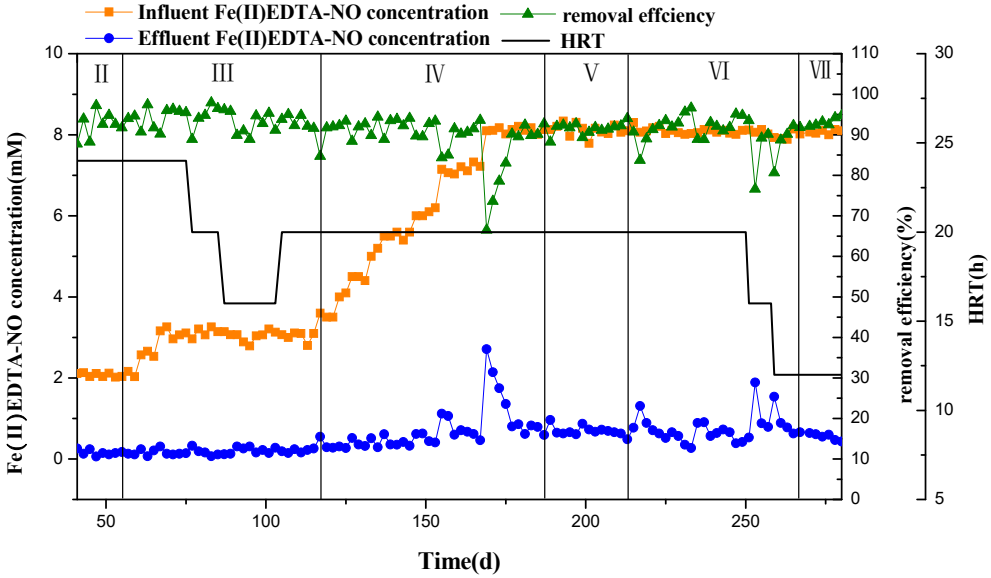

Figure 2. The concentrations of Fe(II)EDTA-NO in the influent and effluent and the Fe(II)EDTA-NO removal efficiency.

After determining the influent concentration of sulfate, HRT was reduced to increase the treatment loads of sulfate and Fe(II)EDTA-NO. Because the influent sulfate concentration was radically high, HRT was reduced by four hours each time. When HRT was reduced from 24 h to 20 h, the removal efficiency of sulfate and Fe(II)EDTA-NO could reach more than 90% (Figure 2). However, when the HRT was reduced to 16 h, the removal efficiency of sulfate radical decreased significantly and the maximum was only 83%. After HRT was restored to 20 h, the sulfate removal efficiency was still 95% and the reactor performance was restored. So, the HRT was maintained at 20 h. After about 120 days of operation of the reactor, the removal load of sulfate was 2.88 kg $SO_4^{2-}\cdot m^{-3}\cdot d^{-1}$. Cunha et al. used an UASB reactor to treat acid mine drainage and the maximum sulfate loading rate was 2.6 g $SO_4^{2-}\cdot L^{-1}\cdot d^{-1}$ [29]. It could be seen that the sulfate treatment load and removal efficiency of this experiment had reached a high level. The removal rate of Fe(II)EDTA-NO was relatively stable in the process of reducing HRT, which proved that the load of Fe(II)EDTA-NO can continue to increase.

In the fourth stage, in order to reduce sulfide content in the effluent, the Fe(II)EDTA-NO concentration in the influent increased by 0.5 mM each adjustment (Figure 2). In the process of increasing the concentration of Fe(II)EDTA-NO from 3 to 8 mM, the sulfate reduction was affected. However, its efficiency could be restored by stable operation and the removal efficiency of Fe(II)EDTA-NO was about 93%. In this stage, the production of sulfide in effluent decreased by about 3 mM during the process of increasing the influent Fe(II)EDTA-NO concentration to 8 mM. Sulfide autotrophic denitrification with Fe(II)EDTA-NO was the main reaction for the removal of sulfide in combination with microbial community analysis. At the same time, the total iron loss increased slightly, about 0.5 mM

(Figure 3). Fe(II)EDTA-NO concentration accounted for about 32% of sulfate concentration, which was within the proportion range of NO and SO_2 in flue gas.

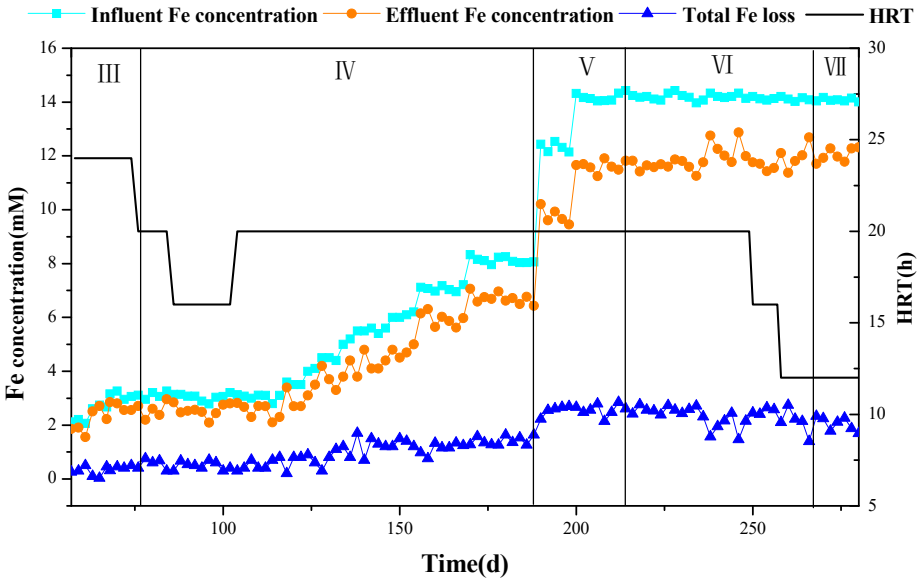

Figure 3. The concentrations of total Fe in the influent and effluent and the total Fe loss.

In the process of NO absorption, Fe(II)EDTA is often oxidized to Fe(III)EDTA by oxygen in flue gas [30]. Therefore, it is necessary to consider how to reduce Fe(III)EDTA to Fe(II)EDTA to ensure the absorption capacity of the solution. Tomasz et al. studied the reduction of Fe(III)EDTA by normal-size zinc, aluminum, tin powders and nano-zinc powders, respectively. It was found that the reduction of Fe(III)EDTA by normal-size zinc powder is faster than that of aluminum and tin powders. The reduction rate of Fe(III)EDTA by nano-zinc powder is about 11 times faster than that of normal-size zinc powder [31,32]. He et al. found that thiourea dioxide can react with Fe(III)EDTA to form Fe(II)EDTA, urea and sulfite [33]. In the study of Sun et al., during absorption of NO with Fe(II)EDTA in the presence of SO_2, the added coal in the solution could inhibit the decrease of Fe^{2+} concentration and increase NO removal efficiency [34]. These methods are all through the addition of chemical agents to complete the regeneration of complexing agent, which undoubtedly increases the cost. As we know, Fe(III)EDTA can react with S^{2-} to form Fe(II)EDTA and S^0 (Equation (6)) [16]. Van der Maas et al. completed the reduction of Fe(III)EDTA by adding 2 mM of Na_2S in the start-up stage of the reactor [35]. When simultaneous flue gas desulfurization and denitrification are carried out in the same reactor, the sulfide produced by sulfate reduction reacts with Fe(III)EDTA to convert sulfide in water into S^0, and the complexing agent can be regenerated without additional reagents. In the fifth stage, the reduction of sulfide by adding Fe(III)EDTA was also studied.

$$2\text{Fe(III)EDTA} + S^{2-} \rightarrow 2\text{Fe(II)EDTA} + S^0 \quad (6)$$

In our experiment, 4 mM Fe(III)EDTA was added firstly and the sulfide content decreased significantly during the process by about 2.8 mM. At the same time, the total iron loss increased by about 0.8 mM (Figure 3) and no Fe(III) was detected in the effluent. The oxidation-reduction reaction between Fe(III) and sulfide may produce elemental sulfur. Continuous addition of 2 mM Fe(III) resulted in a reduction of sulfide concentration by about 0.9 mM and no significant changes in total iron loss. The total iron concentration in the solution was about 14 mM, which was close to the total iron concentration studied by Zhang et al. [36]. Considering that the addition of Fe(III)EDTA would increase the loss of total iron and the inhibition of EDTA on microorganisms, the Fe(III)EDTA concentration no longer increased and was maintained at 6 mM.

The sixth stage was to reduce sulfide production by reducing the concentration of sulfate in the influent. As shown in Figure 1, reduction of sulfate concentration had little effect on sulfate and Fe(II)EDTA-NO removal efficiency, however sulfide concentration in effluent decreased significantly. When the concentration of sulfate in the influent decreased to 15 mM, the average concentration of sulfide in the effluent was 0.9 mM. It was about 4 mM lower than that of the fifth stage. In order to maintain the sulfate treatment load, the HRT was gradually reduced. The reduction efficiency of sulfate and Fe(II)EDTA-NO fluctuated during the reduction of HRT from 20 h to 12 h. However, with the steady operation of the reactor, the sulfate and Fe(II)EDTA-NO removal efficiencies could be restored quickly, which were stable at 96% and 92%, respectively. At this time, the treatment loads of sulfate and Fe(II)EDTA-NO reached 2.88 kg $SO_4^{2-}\cdot m^{-3}\cdot d^{-1}$ and 0.48 kg $NO\cdot m^{-3}\cdot d^{-1}$. The sulfate treatment load was the same as that of the third stage. The Fe(II)EDTA-NO treatment load reached the maximum load after the reactor was started. Van der Maas et al. tested technical feasibility of the BioDeNOx process. It was found that the Fe(II)EDTA-NO removal load was 9.5 mmol $NO\cdot L^{-1}\cdot d^{-1}$ (equal to 0.285 kg $NO\cdot m^{-3}\cdot d^{-1}$) when the NO removal efficiency remained between 70% and 80% [37]. Chandrashekhar et al. used an up-flow packed bed bioreactor (UAPBR) to reduce FeNTA-NO and the reduction efficiency reached 87.8% at a loading rate of 0.24 mmol $NO\cdot L^{-1}\cdot h^{-1}$ (equal to 0.1728 kg $NO\cdot m^{-3}\cdot d^{-1}$) [38]. This demonstrates that the removal load of Fe(II)EDTA-NO reached a high level in our experiment.

3.2. Conversion of Fe and S Elements and Analysis of Reduction Products of Fe(II)EDTA-NO

3.2.1. Conversion Analysis of Fe Elements

In this experiment, the ratio of Fe to EDTA was 1:2 when Fe(II)EDTA was prepared. Under this ratio, Fe(II)EDTA was stable and the precipitation of FeS could be controlled [25].

As can be seen from Figure 3, in the third and fourth stages of reactor operation, the total iron loss was very small when the influent concentration of Fe(II)EDTA-NO was 2–3 mM. This was consistent with the experimental results [13]. When the influent concentration of Fe(II)EDTA-NO reached 8 mM, the loss of Fe increased by about 0.5 mM. No Fe(III) was detected in the effluent of the reactor and the effluent total iron concentration was basically the same as that of the ferrous iron. The dissolved Fe(II) should exist in the form of Fe(II)EDTA.

After adding Fe(III)EDTA in the fifth stage, the total loss of Fe increased by about 1.5 mM. By acid dissolution of the precipitate in the effluent, Fe(II) and Fe(III) were found in the precipitate and the content of Fe(III) was less. It was proved that the precipitate was mainly FeS with a small amount of ferric hydroxide precipitate [26,27,39]. According to the analysis of sulfide concentration change at this stage, it is inferred that the main process is the oxidation–reduction reaction between Fe(III) and sulfide to form Fe(II) and elemental sulfur, accompanied by the formation of a small amount of FeS precipitation. In the sixth stage, the total iron loss did not change significantly with the change of sulfate concentration and HRT.

3.2.2. Analysis of S Element Equilibrium

Analysis of sulfur equilibrium in the seventh stage of reactor (Table 2), sulfite and thiosulfate were not detected in the effluent liquid phase. The presence of hydrogen sulfide was measured in the gas phase of the reactor. According to the analysis of sulfur balance, 4.2% and 8% of sulfur were present in the effluent as sulfates and sulfides. About 10% of the sulfur was transferred to the gas phase H_2S. The remaining 77.8% sulfur was mainly converted to elemental sulfur through sulfur autotrophic denitrification and chemical reaction processes.

Table 2. Element balance analysis of S.

Days/d	Influent Load of SO_4^{2-}-S/kg·m^{-3}·d^{-1}	Load of S^{2-}-S/kg·m^{-3}·d^{-1}	Load of H_2S-S/kg·m^{-3}·d^{-1}	SO_4^{2-} Removal Efficiency/%
1	0.97	0.08	0.13	94.93
2	1.00	0.08	0.17	94.84
3	0.98	0.09	0.02	96.54
4	0.95	0.05	0.11	95.20
5	1.00	0.08	0.01	95.77
6	1.03	0.08	0.15	96.71
7	1.04	0.07	0.04	97.18
8	0.99	0.07	0.13	95.78
9	0.94	0.07	0.14	94.63
10	1.00	0.06	0.15	95.90
11	1.05	0.06	0.15	96.52
12	0.97	0.07	0.13	96.16
average	0.99	0.07	0.11	95.85

Other researchers have proposed that the amount of total sulfur in the reactor influent minus the amount of residual sulfates, thiosulfates and sulfides in the reactor effluent is the amount of elemental sulfur production in the SANI system of co-conversion of sulfates and nitrates [40]. Chen et al. studied the simultaneous removal of NO and SO_2 by rotating drum biofilter coupled with Fe(II)EDTA. Their results showed that sulfide produced by sulfate reduction could be converted into elemental sulfur by sulfur autotrophic denitrification and the sulfide was emitted in the form of hydrogen sulfide at low NO concentration [9,10]. They recommend the sulfur autotrophic denitrification reaction as shown in Equation (7).

$$Fe(II)EDTA\text{-}NO^{2-} + HS^- \rightarrow Fe(II)EDTA^{2-} + 0.5N_2 + S_0 + OH^- \quad (7)$$

In our experiment, 77.8% sulfur was converted to elemental sulfur when the sulfate concentration in the influent was 15 mM. About 11.67 mM elemental sulfur could be formed. According to Equation (6), 6 mM Fe(III)EDTA may generate 3 mM elemental sulfur. Further, 8 mM Fe(II)EDTA-NO may generate 8 mM elemental sulfur if all Fe(II)EDTA-NO was converted by sulfur autotrophic denitrification process (Equation (7)). The elemental sulfur produced theoretically by Equations (6) and (7) was similar to the sulfur equilibrium analysis data in Table 2. The effluent concentration of sulfide in the reactor was very small in the seventh stage, and the production of hydrogen sulfide and ferrous sulfide should be relatively small.

The effluent of the reactor was slightly yellowish (Supplementary Materials Figure S1) and some of the elemental sulfur produced was colloidal and not completely precipitated. The effluent was centrifuged and the sediments were cleaned. After drying, the sediments were detected by liquid chromatography. By comparing the measured results with the chromatogram of standard sulfur, it was found that the sample had the same residence time as sulfur (Figures S2 and S3), which can prove the existence of elemental sulfur in the product.

The final product of sulfate reduction in our experiment was mainly elemental sulfur, which can be applied to industrial and agricultural areas to further reduce costs. Zhang et al. [41] added a sedimentation tank for the recovery of elemental sulfur in the process of treating sulfate-containing wastewater. The recovery rate of elemental sulfur can reach 76%. The influence of sulfur recovery on the operation cost of flue gas desulfurization and denitrification will be carried out in the next research. It has been reported that selenium in flue gas from fuel combustion can be transformed into Se^0 by microorganisms [42]. The synchronous removal and recovery of sulfur, nitrogen, selenium and mercury in flue gas needs to be further studied.

3.2.3. Analysis of Reduction Products of Fe(II)EDTA-NO

The Fe(II)EDTA-NO reduction products were also analyzed in the seventh stage (Table 3). The results showed that no N_2O was found in the gas phase and no nitrate and nitrite were detected in the liquid phase. The influent NO-N load was 0.224 $kg \cdot m^{-3} \cdot d^{-1}$ and the average nitrogen content in the generated N_2 was 0.189 $kg \cdot m^{-3} \cdot d^{-1}$, accounting for 91% of the removal. Therefore, the final product of NO denitrification was mainly N_2.

Table 3. Analysis of reduction products of Fe(II)EDTA-NO.

Days/d	Influent Load of NO-N/$kg \cdot m^{-3} \cdot d^{-1}$	Load of N_2-N/$kg \cdot m^{-3} \cdot d^{-1}$	NO Removal Efficiency/%
1	0.224	0.194	94.3
2	0.226	0.187	92.1
3	0.219	0.186	93.3
4	0.225	0.191	92.4
5	0.224	0.180	90.3
6	0.227	0.196	93.2
7	0.226	0.189	92.1
average	0.224	0.189	92.5

In the BioDeNOx process, the reduction of NO to N_2 was found to be biologically catalyzed with nitrous oxide (N_2O) as an intermediate [43]. They found that the NO (aq) and Fe(II)EDTA concentration had an effect on the accumulation rate of N_2O [44]. Other studies have shown that N_2O accumulation was inhibited with a high C/N ratio, sufficient electron donor and a low sulfite concentration [45]. However, N_2 as the final product of Fe(II)EDTA-NO reduction was recognized by most researchers [7–11,13,20,35,37,38,45–47].

3.3. Analysis of Reactor Microbial Community Structure

Sludge samples from the third, fourth and sixth stages of the reactor operation were taken to analyze the microbial community structure in the reactor.

Five sulfate reducing bacteria, *Desulfomicrobium*, *Desulfomonas*, *Desulfovibrio*, *Desulfobulbus* and *Desulfobacter*, were found in the third stage. Abundance reached 22.53%, 0.7%, 1.05%, 2.81% and 1.15%, respectively (Figure 4). These five bacteria can use organic carbon sources such as sodium lactate to reduce sulfate [48–51] and the dominant strain was *Desulfomicrobium*. A sulfur autotrophic denitrifying bacteria *Sulfurovum* was also found in the system, accounting for 1.39%. *Sulfurovum* can simultaneously oxidize sulfides and reduce nitrates in a chemoautotrophic manner [52,53]. The presence of this bacteria may have played a role in the simultaneous removal of Fe(II)EDTA-NO and sulfide in the reaction system which would produce S^0 and regenerated Fe(II)EDTA. *Pseudomonas* also existed in the reactor, accounting for 3.62%. *Pseudomonas* is a facultative anaerobic bacteria. It has been proved that *Pseudomonas* can reduce Fe(II)EDTA-NO with glucose as a carbon source in the BioDeNOx system [54]. *Pseudomonas* has also been found to use Fe(II)EDTA-NO and sulfide for sulfur autotrophic denitrification and the proportion could reach up to 35.7% [9]. Fermentation acidogenic bacteria *Ornatilinea* and *Cloacibacillus* were also found in the reactor. There were also *Aminivibrio* strains related to amino acid metabolism. *Methanothrix* can decompose acetic acid with sulfide as a sulfur source to produce CH_4 and CO_2 [55]. *Tissierella* can metabolize protein, yeast extract and glucose and produce hexanoic acid, propionic acid, isohydric acid, T acid, isovaleric acid and other low molecular organic acids (or volatile fatty acids) [56].

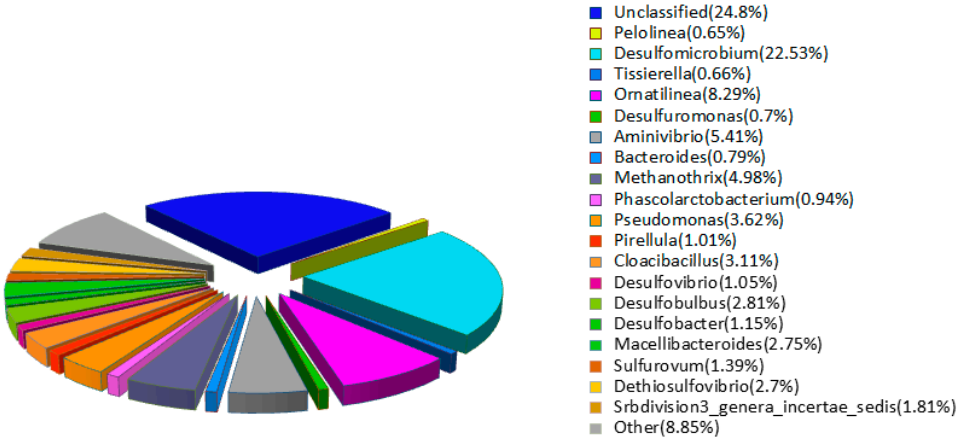

Figure 4. Analysis of microbial community structure in the third stage of the reactor.

In the fourth stage, the species and abundance of sulfate reducing bacteria did not change much in the reactor. The proportion of *Pseudomonas* increased by 5.06%, and that of *Sulfurovum* increased by 3.95%. In the fourth stage, two other sulfur oxidizing bacteria, *Alcaligenes* and *Arobacter*, were found with abundances of 0.74% and 0.73%, respectively (Figure 5). *Alcaligenes* is a colorless sulfur bacteria which can obtain energy from redox sulfur compounds under the condition of heterotrophy of chemical energy [57]. *Arcobacter* can use nitrate or molecular oxygen as electron acceptors to redox sulfur compounds and obtain the energy needed for growth [58]. With the increase of the Fe(II)EDTA-NO concentration in the influent, the increase of the proportion of *Pseudomonas* and *Sulfurovum* and the discovery of *Arobacter* may promote the sulfur autotrophic denitrification process. This may have played a role in the reduction of sulfide concentration.

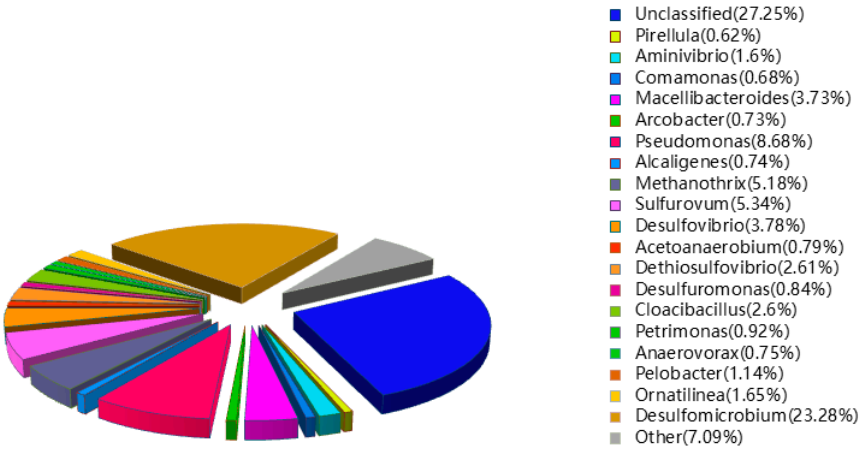

Figure 5. Analysis of microbial community structure in the fourth stage of the reactor.

In the sixth stage, the dominant bacteria were *Desulfomicrobium* (19.76%) and *Pseudomonas* (8.7%). Several other sulfate reducing bacteria, including *Desulfomonas*, *Desulfovibrio* and *Desulfobacter*, accounted for 6.22% of the total (Figure 6). The proportion of *Pseudomonas* slightly increased compared with the fourth stage. It may be that the addition of Fe(II)EDTA-NO load promotes the growth of *Pseudomonas*. *Sulfurovum* accounted for 4.49 % of the total which slightly decreased compared with the fourth stage. At the same time, a heterotrophic desulfurization and nitrogen fixing bacteria *Azoarcus* (1.77%) was found, which can oxidize sulfide to sulfur in a weak alkaline environment [59].

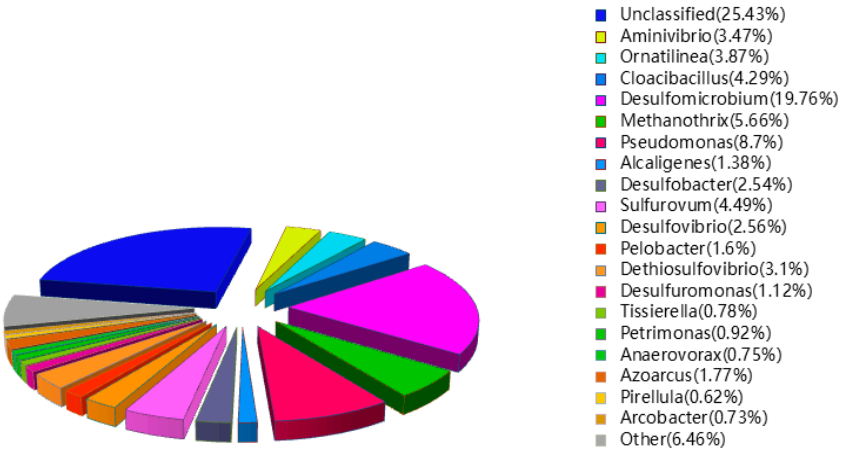

Figure 6. Analysis of microbial community structure in the sixth stage of the reactor.

4. Conclusions

The simultaneous reduction of sulfate and Fe(II)EDTA-NO in an anaerobic moving-bed biofilm reactor was carried out. When the influent loads of sulfate and Fe(II)EDTA-NO were 2.88 kg $SO_4^{2-}\cdot m^{-3}\cdot d^{-1}$ and 0.48 kg $NO\cdot m^{-3}\cdot d^{-1}$, the removal efficiency of the two substances reached 96% and 92%, respectively. By increasing the concentration of Fe(II)EDTA-NO in the influent and adding Fe(III)EDTA, the sulfide concentration in the effluent could be reduced through sulfur autotrophic denitrification and chemical reaction. Further, the reduction products of sulfate were mainly in the form of elemental sulfur. The final product of Fe(II)EDTA-NO removal was N_2. Through the analysis of microbial community in the reactor, it was found that the dominant strain of sulfate reducing bacteria in the system was *Desulfomicrobium*. The reduction process of Fe(II)EDTA-NO mainly depends on *Pseudomonas*. *Sulfurovum* and *Arcobacter* were also found in the system. Through the sulfur autotrophic denitrification process, they can remove Fe(II)EDTA-NO and reduce sulfide concentration at the same time.

Supplementary Materials: The following are available online at http://www.mdpi.com/2075-163X/9/6/330/s1, Figure S1: The color contrast of the reactor effluent and tap water; Figure S2: HPLC of sulfur (standard sulfur); Figure S3: HPLC of sample (the reactor effluent).

Author Contributions: Conceptualization, Y.Z.; Methodology, Y.Z.; Validation, Y.Z.; Formal Analysis, L.S.; Investigation, L.S.; Resources, Y.Z. and J.Z.; Data Curation, L.S.; Writing—original draft preparation, L.S.; Writing—review and editing, Y.Z.; Visualization, L.S. and Y.Z.; Supervision, J.Z.; Project administration, Y.Z.

Funding: The work was supported by National Natural Science Foundation of China (No. 51578106), the Fundamental Research Funds for the Central Universities (No. DUT18ZD215).

Conflicts of Interest: The authors declare no conflict of interest.

References

1. Cazorla, M. Air quality over a populated Andean region: Insights from measurements of ozone, NO, and boundary layer depths. *Atmos. Pollut. Res.* **2016**, *7*, 66–74. [CrossRef]
2. Hao, R.L.; Zhao, Y.; Yuan, B.; Zhou, S.H.; Yang, S. Establishment of a novel advanced oxidation process for economical and effective removal of SO_2 and NO. *J. Hazard. Mater.* **2016**, *318*, 224–232. [CrossRef] [PubMed]
3. Wei, Z.S.; Huang, Q.R.; Wang, J.B.; Huang, Z.S.; Chen, Z.Y.; Li, B.R. Performance and mechanism of nitric oxide removal using a thermophilic membrane biofilm reactor. *Fuel Process. Technol.* **2016**, *148*, 217–223. [CrossRef]
4. Wang, X.C.; Bi, X.Y.; Sun, P.S.; Chen, J.Q.; Zou, P.; Ma, X.M.; Zhang, J.; Wang, H.Y.; Xu, X.Y. Effects of oxygen content on the simultaneous microbial removal of SO_2 and NOx in biotrickling towers. *Biotechnol. Bioprocess. Eng.* **2015**, *20*, 924–930. [CrossRef]
5. Pandey, R.A.; Biswas, R.; Chakrabarti, T.; Devotta, S. Flue gas desulfurization: Physicochemical and biotechnological approaches. *Crit. Rev. Environ. Sci. Technol.* **2005**, *35*, 571–622. [CrossRef]

6. Wang, J.; Cao, Y.; Zhong, Q. Formulation and optimization of biological removal of flue gas pretreatment wastewater and sulfur recycling process by Box-Behnken design. *Water Sci. Technol.* **2013**, *67*, 2706–2711. [CrossRef] [PubMed]
7. Li, W.; Li, M.F.; Zhang, L.; Zhao, J.K.; Xia, Y.F.; Liu, N.; Li, S.J.; Zhang, S.H. Enhanced NOx removal performance and microbial community shifts in an oxygen-resistance chemical absorption-biological reduction integrated system. *Chem. Eng. J.* **2016**, *290*, 185–192. [CrossRef]
8. Zhou, Z.M.; Jing, G.H.; Zhou, Q. Enhanced NOx removal from flue gas by an integrated process of chemical absorption coupled with two-stage biological reduction using immobilized microorganisms. *Process Saf. Environ. Prot.* **2013**, *91*, 325–332. [CrossRef]
9. Chen, J.; Gu, S.-Y.; Zheng, J.; Chen, J.-M. Simultaneous removal of SO_2 and NO in a rotating drum biofilter coupled with complexing absorption by Fe(II)EDTA. *Biochem. Eng. J.* **2016**, *114*, 90–96. [CrossRef]
10. Chen, J.; Li, B.; Zheng, J.; Chen, J. Control of H_2S generation in simultaneous removal of NO and SO_2 by rotating drum biofilter coupled with FeII(EDTA). *Environ. Technol.* **2019**, *40*, 1576–1584. [CrossRef]
11. Chen, M.X.; Zhang, Y.; Zhou, J.T.; Dong, X.Y.; Wang, X.J.; Shi, Z. Sulfate removal by Desulfovibrio sp CMX in chelate scrubbing solutions for NO removal. *Bioresour. Technol.* **2013**, *143*, 455–460. [CrossRef] [PubMed]
12. Chen, M.X.; Zhou, J.T.; Zhang, Y.; Wang, X.J.; Shi, Z.; Wang, X.W. Fe(III)EDTA and Fe(II)EDTA-NO reduction by a sulfate reducing bacterium in NO and SO_2 scrubbing liquor. *World J. Microbiol. Biotechnol.* **2015**, *31*, 527–534. [CrossRef] [PubMed]
13. Zhang, Y.; Wan, F.; Zhou, J.T. Anaerobic reduction process characteristics and microbial community analysis for sulfate and fe(II)edta-no/fe(III) edta. *Environ. Sci.* **2017**, *38*, 4706–4714. [CrossRef]
14. Manconi, I.; van der Maas, P.; Lens, P.N.L. Effect of sulfur compounds on biological reduction of nitric oxide in aqueous Fe(II)$EDTA^{2-}$ solutions. *Nitric Oxide-Biology Chem.* **2006**, *15*, 40–49. [CrossRef] [PubMed]
15. Velasco, A.; Morgan-Sagastume, J.M.; Gonzalez-Sanchez, A. Evaluation of a hybrid physicochemical/biological technology to remove toxic H_2S from air with elemental sulfur recovery. *Chemosphere* **2019**, *222*, 732–741. [CrossRef] [PubMed]
16. Miao, X.M.; Ma, Y.W.; Chen, Z.Z.; Gong, H.J. Oxidative degradation stability and hydrogen sulfide removal performance of dual-ligand iron chelate of Fe-EDTA/CA. *Environ. Technol.* **2018**, *39*, 3006–3012. [CrossRef] [PubMed]
17. Biswas, K.; Taylor, M.W.; Turner, S.J. dsrAB-based analysis of sulphate-reducing bacteria in moving bed biofilm reactor (MBBR) wastewater treatment plants. *Appl. Microbiol. Biotechnol.* **2014**, *98*, 7211–7222. [CrossRef] [PubMed]
18. Zhang, S.H.; Chen, H.; Xia, Y.F.; Zhao, J.K.; Liu, N.; Li, W. Re-acclimation performance and microbial characteristics of a thermophilic biofilter for NOx removal from flue gas. *Appl. Microbiol. Biotechnol.* **2015**, *99*, 6879–6887. [CrossRef] [PubMed]
19. Yuan, Q.; Wang, H.Y.; Hang, Q.Y.; Deng, Y.F.; Liu, K.; Li, C.M.; Zheng, S.Z. Comparison of the MBBR denitrification carriers for advanced nitrogen removal of wastewater treatment plant effluent. *Environ. Sci. Pollut. Res.* **2015**, *22*, 13970–13979. [CrossRef] [PubMed]
20. Li, N.; Zhang, Y.; Li, Y.M.; Chen, M.X.; Dong, X.Y.; Zhou, J.T. Reduction of Fe(II)EDTA-NO using *Paracoccus denitrificans* and changes of Fe(II)EDTA in the system. *J. Chem. Technol. Biotechnol.* **2013**, *88*, 311–316. [CrossRef]
21. APHA; AWWA; WEF. *Standard Methods for the Examination of Water and Wastewater*, 21st ed.; American Public Health Association: Washington, DC, USA, 2005.
22. Chen, M.J.; Zhang, Z.; Bott, T.R. Effects of operating conditions on the adhesive strength of Pseudomonas fluorescens biofilms in tubes. *Colloids Surf. B* **2005**, *43*, 61–71. [CrossRef]
23. Abtahi, S.M.; Petermann, M.; Flambard, A.J.; Beaufort, S.; Terrisse, F.; Trotouin, T.; Cassan, C.J.; Albasi, C. Micropollutants removal in tertiary moving bed biofilm reactors (MBBRs): Contribution of the biofilm and suspended biomass. *Sci. Total Environ.* **2018**, *643*, 1464–1480. [CrossRef]
24. Lin, S.; Mackey, H.R.; Hao, T.-W.; Guo, G.; van Loosdrecht, M.C.M.; Chen, G.-H. Biological sulfur oxidation in wastewater treatment: A review of emerging opportunities. *Water Res.* **2018**, *143*, 399–415. [CrossRef]
25. Wang, X.J.; Zhang, Y.; Dong, X.Y.; Chen, M.X.; Shi, Z.; Zhou, J.T. Fe(II)EDTA-NO reduction by sulfide in the anaerobic aqueous phase: stoichiometry and kinetics. *Energy Fuels* **2013**, *27*, 6024–6030. [CrossRef]

26. Zhou, C.; Zhou, Y.; Rittmann, B.E. Reductive precipitation of sulfate and soluble Fe(III) by Desulfovibrio vulgaris: Electron donor regulates intracellular electron flow and nano-FeS crystallization. *Water Res.* **2017**, *119*, 91–101. [CrossRef]
27. Xia, D.; Yi, X.Y.; Lu, Y.; Huang, W.L.; Xie, Y.Y.; Ye, H.; Dang, Z.; Tao, X.Q.; Li, L.; Lu, G.N. Dissimilatory iron and sulfate reduction by native microbial communities using lactate and citrate as carbon sources and electron donors. *Ecotoxicol. Environ. Saf.* **2019**, *174*, 524–531. [CrossRef] [PubMed]
28. Saritpongteeraka, K.; Chaiprapat, S. Effects of pH adjustment by parawood ash and effluent recycle ratio on the performance of anaerobic baffled reactors treating high sulfate wastewater. *Bioresour. Technol.* **2008**, *99*, 8987–8994. [CrossRef] [PubMed]
29. Cunha, M.P.; Ferraz, R.M.; Sancinetti, G.P.; Rodriguez, R.P. Long-term performance of a UASB reactor treating acid mine drainage: effects of sulfate loading rate, hydraulic retention time, and COD/SO_4^{2-} ratio. *Biodegradation* **2019**, *30*, 47–58. [CrossRef] [PubMed]
30. He, F.Q.; Deng, X.H.; Chen, M. Kinetics of FeIIIEDTA complex reduction with iron powder under aerobic conditions. *RSC Adv.* **2016**, *6*, 38416–38423. [CrossRef]
31. Augustyniak, A.W.; Suchecki, T.T.; Kumazawa, H. Reactivity of nano-size zinc powder in the aqueous solution of $[Fe^{III}(edta)(H_2O)]^-$. *Environ. Technol.* **2017**, *38*, 103–107. [CrossRef]
32. Suchecki, T.T.; Mathews, B.; Augustyniak, A.W.; Kumazawa, H. Applied kinetics aspects of ferric EDTA complex reduction with metal powder. *Ind. Eng. Chem. Res.* **2014**, *53*, 14234–14240. [CrossRef]
33. He, F.; Qian, Y.; Xu, J. Performance, mechanism, and kinetics of Fe(III)EDTA reduction by thiourea dioxide. *Energy Fuels* **2019**, *33*, 3331–3338. [CrossRef]
34. Sun, W.; Zhou, J.; Chen, J. Removal of nitric oxide using combined Fe(II)EDTA and coal slurry in the presence of SO_2. *Sep. Purif. Technol.* **2017**, *188*, 134–139. [CrossRef]
35. Van der Maas, P.; van den Brink, P.; Utomo, S.; Klapwijk, B.; Lens, P. NO removal in continuous BioDeNOx reactors: Fe(II)$EDTA^{2-}$ regeneration, biomass growth, and EDTA degradation. *Biotechnol. Bioeng.* **2006**, *94*, 575–584. [CrossRef]
36. Zhang, R.; Wang, L.T.; Chen, P.; Pu, Y.W. Shifts in microbial community structure and diversity in a novel waterfall biofilm reactor combined with MBBR under light and dark conditions. *Rsc Adv.* **2018**, *8*, 37462–37471. [CrossRef]
37. Van der Maas, P.; van den Bosch, P.; Klapwijk, B.; Lens, P. NOx removal from flue gas by an integrated physicochernical absorption and biological denitrification process. *Biotechnol. Bioeng.* **2005**, *90*, 433–441. [CrossRef]
38. Chandrashekhar, B.; Sahu, N.; Tabassum, H.; Pai, P.; Morone, A.; Pandey, R.A. Treatment of ferrous-NTA-based NO(x) scrubber solution by an up-flow anaerobic packed bed bioreactor. *Appl. Microbiol. Biotechnol.* **2015**, *99*, 5281–5293. [CrossRef]
39. Johnson, D. Recent developments in microbiological approaches for securing mine wastes and for recovering metals from mine waters. *Minerals* **2014**, *4*, 279–292. [CrossRef]
40. Xu, X.J.; Chen, C.; Wang, A.J.; Yu, H.; Zhou, X.; Guo, H.L.; Yuan, Y.; Lee, D.J.; Zhou, J.; Ren, N.Q. Bioreactor performance and functional gene analysis of microbial community in a limited-oxygen fed bioreactor for co-reduction of sulfate and nitrate with high organic input. *J. Hazard. Mater.* **2014**, *278*, 250–257. [CrossRef]
41. Zhang, Y.; Zhang, L.; Li, L.; Chen, G.-H.; Jiang, F. A novel elemental sulfur reduction and sulfide oxidation integrated process for wastewater treatment and sulfur recycling. *Chem. Eng. J.* **2018**, *342*, 438–445. [CrossRef]
42. Cordoba, P.; Staicu, L.C. Flue gas desulfurization effluents: An unexploited selenium resource. *Fuel* **2018**, *223*, 268–276. [CrossRef]
43. Van der Maas, P.; van de Sandt, T.; Klapwijk, B.; Lens, P. Biological reduction of nitric oxide in aqueous Fe(II)EDTA solutions. *Biotechnol. Prog.* **2003**, *19*, 1323–1328. [CrossRef]
44. Van der Maas, P.; Manconi, I.; Klapwijk, B.; Lens, P. Nitric oxide reduction in BioDeNOx reactors: Kinetics and mechanism. *Biotechnol. Bioeng.* **2008**, *100*, 1099–1107. [CrossRef]
45. Chen, J.; Wang, J.; Zheng, J.; Chen, J. Prediction and inhibition of the N_2O accumulation in the BioDeNOx process for NOx removal from flue gas. *Bioprocess Biosyst. Eng* **2016**, *39*, 1859–1865. [CrossRef]
46. Chen, J.; Wu, J.-L.; Wang, J.; Zhang, S.-H.; Chen, J.-M. A mass-transfer model of nitric oxide removal in a rotating drum biofilter coupled with Fe(II)EDTA absorption. *Ind. Eng. Chem. Res* **2018**, *57*, 8144–8151. [CrossRef]

47. Zhao, J.K.; Zhang, C.Y.; Sun, C.; Li, W.; Zhang, S.H.; Li, S.J.; Zhang, D.X. Electron transfer mechanism of biocathode in a bioelectrochemical system coupled with chemical absorption for NO removal. *Bioresour. Technol.* **2018**, *254*, 16–22. [CrossRef]
48. Rajeev, L.; Chen, A.; Kazakov, A.E.; Luning, E.G.; Zane, G.M.; Novichkov, P.S.; Wall, J.D.; Mukhopadhyaya, A. Regulation of nitrite stress response in *Desulfovibrio vulgaris* hildenborough, a model sulfate-reducing bacterium. *J. Bacteriol.* **2015**, *197*, 3400–3408. [CrossRef] [PubMed]
49. Dias, M.; Salvado, J.C.; Monperrus, M.; Caumette, P.; Amouroux, D.; Duran, R.; Guyoneaud, R. Characterization of *Desulfomicrobium salsuginis* sp nov and *Desulfomicrobium aestuarii* sp nov., two new sulfate-reducing bacteria isolated from the Adour estuary (French Atlantic coast) with specific mercury methylation potentials. *Syst. Appl. Microbiol.* **2008**, *31*, 30–37. [CrossRef]
50. Wei, L.; Ma, F.; Zhao, G. Composition and dynamics of sulfate-reducing bacteria during the waterflooding process in the oil field application. *Bioresour. Technol.* **2010**, *101*, 2643–2650. [CrossRef]
51. Baldwin, S.; Mattes, A.; Rezadehbashi, M.; Taylor, J. Seasonal microbial population shifts in a bioremediation system treating metal and sulfate-rich seepage. *Minerals* **2016**, *6*, 36. [CrossRef]
52. Xu, J.L.; Fan, Y.M.; Li, Z.X. Effect of pH on elemental sulfur conversion and microbial communities by autotrophic simultaneous desulfurization and denitrification. *Environ. Technol.* **2016**, *37*, 3014–3023. [CrossRef]
53. Huang, C.; Zhao, Y.K.; Li, Z.L.; Yuan, Y.; Chen, C.; Tan, W.B.; Gao, S.; Gao, L.F.; Zhou, J.Z.; Wang, A.J. Enhanced elementary sulfur recovery with sequential sulfate-reducing, denitrifying sulfide-oxidizing processes in a cylindrical-type anaerobic baffled reactor. *Bioresour. Technol.* **2015**, *192*, 478–485. [CrossRef] [PubMed]
54. Zhang, S.H.; Li, W.; Wu, C.Z.; Chen, H.; Shi, Y. Reduction of Fe(II)EDTA-NO by a newly isolated Pseudomonas sp strain DN-2 in NOx scrubber solution. *Appl. Microbiol. Biotechnol.* **2007**, *76*, 1181–1187. [CrossRef] [PubMed]
55. Jetten, M.S.M.; Stams, A.J.M.; Zehnder, A.J.B. Methanogenesis from acetate - a comparison of the acetate metabolism in *Methanothrix-soehngenii* and *methanosarcina* spp. *FEMS Microbiol. Lett.* **1992**, *88*, 181–197. [CrossRef]
56. Collins, M.D.; Shah, H.N. NOTES: Reclassification of *Bacteroides praeacutus* Tissier (Holdeman and Moore) in a New Genus, *Tissierella*, as *Tissierella praeacuta* comb. nov. *Int. J. Syst.* **1986**, *36*, 461–463. [CrossRef]
57. Robertson, L.A.; Kuenen, J.G. The Colorless Sulfur Bacteria. In *The Prokaryotes*; Dworkin, M., Falkow, S., Rosenberg, E., Schleifer, K.-H., Stackebrandt, E., Eds.; Springer: New York, NY, USA, 2006; Volume 2, pp. 975–1011.
58. Garcia-de-Lomas, J.; Corzo, A.; Carmen Portillo, M.; Gonzalez, J.M.; Andrades, J.A.; Saiz-Jimenez, C.; Garcia-Robledo, E. Nitrate stimulation of indigenous nitrate-reducing, sulfide-oxidising bacterial community in wastewater anaerobic biofilms. *Water Res.* **2007**, *41*, 3121–3131. [CrossRef]
59. Garcia-de-Lomas, J.; Corzo, A.; Carmen Portillo, M. *Azoarcus taiwanensis* sp nov., a denitrifying species isolated from a hot spring. *Appl. Microbiol. Biotechnol.* **2014**, *98*, 1301–1307. [CrossRef]